Hindawi
Journal of Electrical and Computer Engineering
Volume 2023, Article ID 7932117, 12 pages
https://doi.org/10.1155/2023/7932117

Research Article

Sliding Mode Control Based on High Gain Observer for Electro-Hydraulic Servo System

Zhenshuai Wan, Yu Fu, Chong Liu, and Longwang Yue

School of Mechanical and Electrical Engineering, Henan University of Technology, Zhengzhou 450001, China

Correspondence should be addressed to Zhenshuai Wan; wanzhenshuai@haut.edu.cn

Received 18 October 2022; Revised 23 December 2022; Accepted 26 December 2022; Published 3 January 2023

Academic Editor: Chao Zhai

The electro-hydraulic servo system is widely used in industrial automation fields for its merits of the high force to weight ratio, compact size, and fast response. However, the parameter uncertainties and external disturbances of the electro-hydraulic servo system significantly deteriorate the control performance of conventional linear controller in practice. To deal with this problem, sliding mode controller (SMC) that incorporates high gain observer (HGO) is proposed in this paper. HGO is used to obtain the accurate time derivative of position signal for sliding mode controller design. The stability of the control system is guaranteed by Lyapunov stability theory. Comparation simulation is conducted to validate the effectiveness of the presented control scheme.

1. Introduction

The electro-hydraulic servo system is widely applied in industrial automation fields, such as aircraft actuator [1], shaking table [2], and construction machine [3], owing to the superiorities such as fast dynamic response, small size, and large force/torque output [4–7]. However, inherent nonlinear friction, parameter variation, and external disturbance restrict the high performance trajectory tracking in practical application [8]. Hence, how to cope with the influence of these drawbacks has attracted the attentions of academia and industry. Although the classical proportional-integral-derivative (PID) controller is widely used in process control, it cannot achieve satisfactory tracking performance when facing the time-varying working condition. To improve the tunning processes of PID, some self-tuning and adaptive strategies have been proposed, such as automatic recalibration features and the hybrid swarm intelligent optimization-PID algorithm [9].

Recently, many advanced control methods have been developed for the hydraulic servo system, such as adaptive control [10–12], backstepping control [13, 14], fuzzy logic (FL) control [15–17], neural network (NN) control [18, 19], and SMC [20–22]. Adaptive control can mitigate parametric variation by using its self-learning properties. Yao et al. used adaptive control to handle the parametric uncertainties and nonlinear friction of hydraulic actuators, where a continuously differentiable nonlinear friction model is first established [23]. However, the tedious adjustment design of control law complicates the controller application. Due to the nonlinear dynamics of hydraulic cylinder and uncertain fluid parameters, backstepping control has been widely used in the hydraulic system. Guo et al. proposed a backstepping controller with extended-state-observer to compensate the unknown load disturbance and uncertain nonlinearity of the electro-hydraulic system [24]. However, the "explosion of complexity" problem restricts its applications. Hence, dynamic surface control technique is integrated into backstepping control to eliminate abovementioned drawbacks and achieve good dynamic tracking performance. To measure the full state variables of the electro-hydraulic system, Kim et al. designed an output feedback nonlinear controller based on backstepping to deal with the unknown external load [25]. However, the aforementioned methods assume the external load disturbance as a known value for ensuring the derivative of Lyapunov function to be negative. To address unknown nonlinear dynamics of the hydraulic servo system, numerous FL- or NN-based control schemes have been constructed. Yang et al. proposed NN-based adaptive dynamic surface controller to improve the transient tracking performance of hydraulic manipulator, where the NN is adopted to approximate the unknown joint coupling dynamics [26–28]. Despite the conceptual simplicity and easy implementation of NN approach, the convergence rates of the NN weights can be very slow. Shen et al. developed a novel fuzzy robust nonlinear controller for electro-hydraulic flight motion simulator, where FL compensator is introduced to estimate nonlinear uncertain functions caused by leakage and bulk modulus [29]. However, the complex design of membership function and fuzzy rules limits its practical application.

As a robust control scheme, SMC can guarantee the robustness of the system with external disturbances, uncertainties, and highly nonlinear characteristics [30]. Nevertheless, the inevitable chattering may lead to the high-frequency activities of the servo valve and then degrade the control performance. To restrain chattering and improve dynamic properties, Cheng et al. presented an observer-based sliding mode control method to tackle the uncertain nonlinearities, external disturbances, and immeasurable states of the electro-hydraulic servo system [31]. However, the velocity and the equivalent pressure of the hydraulic servo system are difficult to obtain online. The high gain observer can provide accurate time derivative information for a given signal, which is important for practical engineering. Won et al. proposed SMC based on HGO for position tracking of the electro-hydraulic servo system, where the velocity and load pressure were estimated by using the position feedback [32]. Motivated by above-mentioned discussions, a novel sliding mode controller based on high gain observer (SMC-HGO) is proposed to deal with parameter uncertainties and external disturbances for the electro-hydraulic servo system.

The rest of the paper is organized as follows: Section 2 describes the electro-hydraulic servo system dynamic model. Subsequently, the controller design is presented in Section 3. The simulation comparisons are presented in Section 4. Finally, Section 5 concludes the paper.

2. Problem Formulation

The electro-hydraulic servo system is comprised of servo valve, hydraulic cylinder, pump, motor, and relief valve. The pump driven by motor delivers the hydraulic oil from the oil tank to servo valve. The relief valve reduces the inlet pressure to a required value and automatically maintains the outlet pressure by returning a required additional amount of flow to the oil tank. The hydraulic cylinder controlled by servo valve converts hydraulic energy into mechanical energy for driving the load movement. The position and torque meter data are collected through the different installed sensors. The control signal generated by the controller actuates the servo valve spool to the proper position. The schematic diagram of the electro-hydraulic servo system is shown in Figure 1.

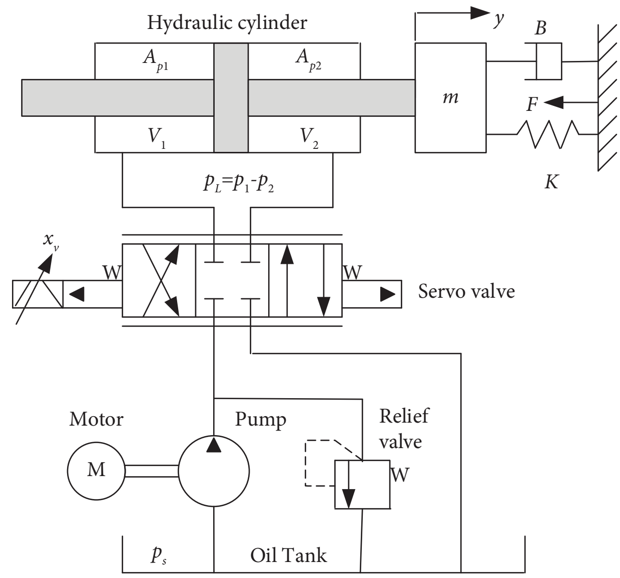

Figure 1: Schematic diagram of the electro-hydraulic servo system.

The dynamics of the electro-hydraulic servo system can be represented as follows [15]:

$$\begin{cases} Ap_L = m\dfrac{\mathrm{d}y}{\mathrm{d}t} + B\dfrac{\mathrm{d}y}{\mathrm{d}t} + Ky \\ Q_L = A\dfrac{\mathrm{d}y}{\mathrm{d}t} + C_{tc}p_L + \dfrac{V_t}{4\beta_e}\dfrac{p_L}{dt} \\ Q_L = C_d w x_v \sqrt{\dfrac{p_s - \operatorname{sign}(x_v)p_L}{\rho}}, \end{cases} \tag{1}$$

where A is the effective area of the cylinder, y is the stroke of the piston position, p_L is the return pressure, m is the mass of the piston, K is the load spring constant, B is the viscous damping coefficient, Q_L is the load flow, C_{tc} is the total leakage coefficient, V_t is the actuator volume, β_e is the effective bulk modulus, C_d is the flow discharge coefficient, w is the area gradient of the servo valve, ρ is the fluid oil density, p_s is the supply pressure, and x_v is the spool position of the servo valve.

Considering equation (1) and selecting displacement y, velocity $\dot{y}$, and acceleration $\ddot{y}$ as the state variables, i.e, $\mathrm{x} = [x_1, x_2, x_3]^T = [y, \dot{y}, \ddot{y}]^T$, the dynamics of electro-hydraulic servo systems can be given as the following state space description:

$$\begin{cases} \dot{x}_1 = x_2 \\ \dot{x}_2 = x_3 \\ \dot{x}_3 = \alpha(x) + g(x_v)u + d, \end{cases} \tag{2}$$

where $\alpha(x) = f_1x_1 + f_2x_2 + f_3x_3$, $f_1 = -4\beta_e C_{tc}K/(mV_t)$, $f_2 = -K/m - 4\beta_e(A^2 + C_{tc}B)/(mV_t)$, $f_3 = -B/m - 4\beta_e C_{tc}/V_t$, $g(x_v) = 4A\beta_e C_d w x_v K_{sv}K_a\sqrt{p_s - p_L\operatorname{sgn}(x_v)}/(mV_t\sqrt{\rho})$,

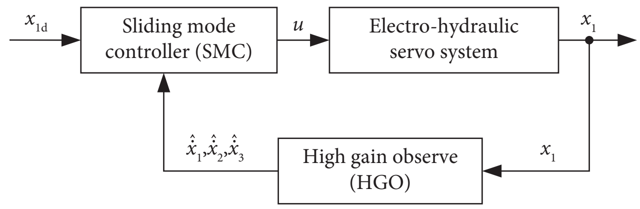

FIGURE 2: Block diagram of the presented SMC-HGO control scheme.

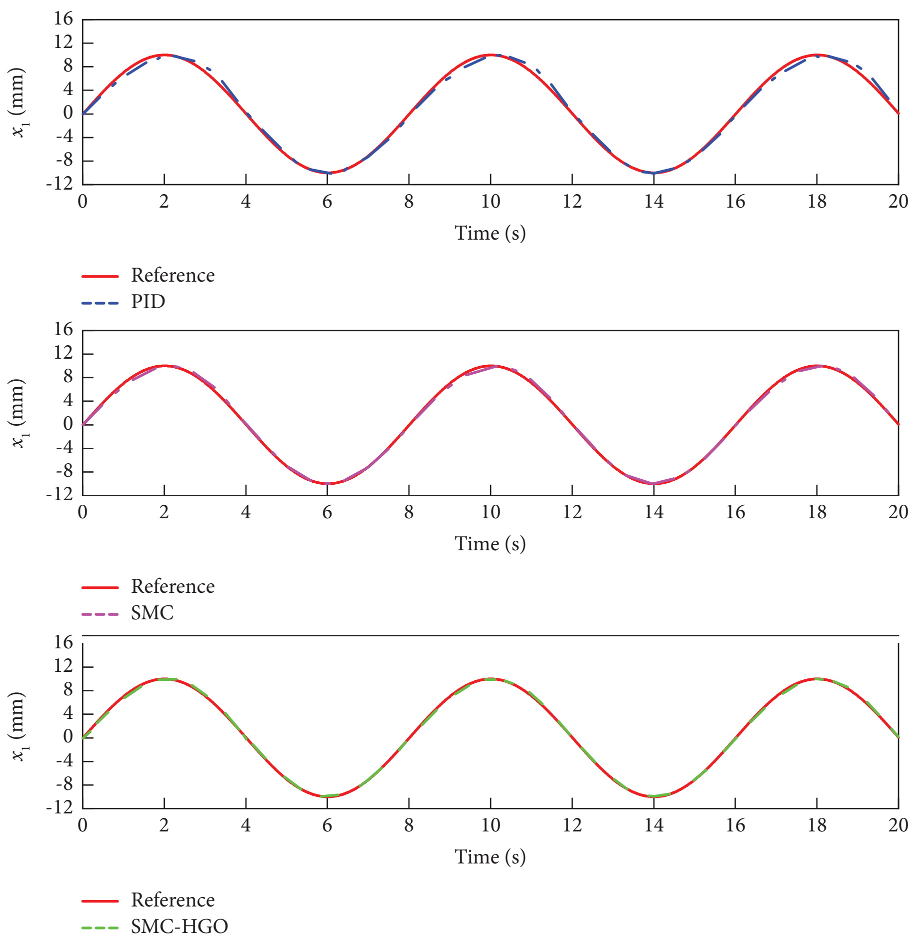

FIGURE 3: Comparative tracking performance of sinusoidal signal.

d is the lumped uncertainties including nonlinear characteristic and external disturbance.

3. Controller Design

The main objective of controller design is to design a robust controller to track a desired trajectory as closely as possible. The HGO with finite time convergence is used to reconstruct velocity and acceleration signal, which will be used in the control design.

The sliding mode function is defined as

$$s = c_1 e + c_2 \dot{e} + \ddot{e}, \tag{3}$$

where $c_1$and c_2 are positive constants, $e = x_1 - x_{1d}$.

The derivative of sliding mode function is

$$\begin{aligned} \dot{s} &= c_1 \dot{e} + c_2 \ddot{e} + \dddot{e} = c_1 \dot{e} + c_2 \ddot{e} + \dddot{x}_1 - \dddot{x}_{1d} \\ &= c_1 \dot{e} + c_2 \ddot{e} + \alpha(x) + g(x_v) u - \dddot{x}_{1d}. \end{aligned} \tag{4}$$

The three-order HGO based on equation (2) is as follows:

$$\begin{cases} \dot{\hat{x}}_1 = x_2 - \dfrac{k_1}{\varepsilon}\left(\hat{x}_1 - x_1(t)\right) \\ \dot{\hat{x}}_2 = x_3 - \dfrac{k_2}{\varepsilon^2}\left(\hat{x}_1 - x_1(t)\right) \\ \dot{\hat{x}}_3 = -\dfrac{k_3}{\varepsilon^3}\left(\hat{x}_1 - x_1(t)\right). \end{cases} \tag{5}$$

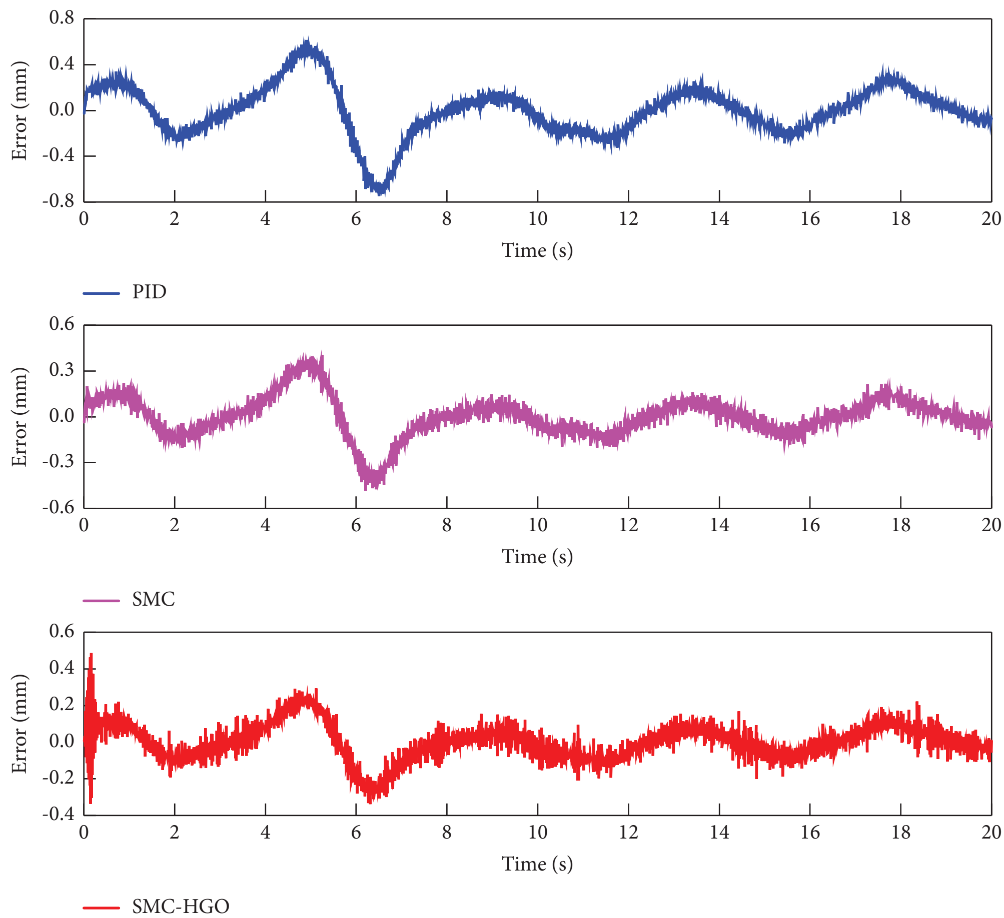

FIGURE 4: Comparative tracking errors of sinusoidal signal.

Where k_1, k_2, and k_3 are positive constants, $\varepsilon << 1$. It should be noted that the gains of HGO largely determines the performance of the controller. Thus, it is important to properly design the gains of HGO to avoid the control input saturation.

We define $h_1 = k_1/\varepsilon$, $h_2 = k_2/\varepsilon^2$, $h_3 = k_3/\varepsilon^3$, and the differentiator is presented as

$$\begin{cases} \dot{\tilde{x}}_1 = \tilde{x}_2 - h_1\tilde{x}_1 \\ \dot{\tilde{x}}_2 = \tilde{x}_3 - h_2\tilde{x}_1 \\ \dot{\tilde{x}}_3 = -h_3\tilde{x}_1. \end{cases} \tag{6}$$

The SMC-HGO is designed as

$$u(t) = \frac{1}{g(x_v)}\left(-c_1\dot{\hat{e}} - c_2\ddot{\hat{e}} - \alpha(\hat{x}) - \eta\hat{s} + \dddot{x}_{1d}\right), \tag{7}$$

where $\hat{e} = \hat{x}_1 - x_{1d}$, $\hat{s} = c_1\hat{e} + c_2\dot{\hat{e}} + \ddot{\hat{e}}$.

It is important to note that the sliding mode surface s is discontinuity function, because it contains sgn $(\cdot)$ function of $g(x_v)$. For eliminating the chattering phenomena, the traditional sign function sgn (x) in $g(x_v)$ is replaced by hyperbolic tangent function tanh (kx), where the positive constant k is much larger than zero.

Then, the derivative of s is written as

$$\begin{aligned} \dot{s} &= c_1\dot{e} + c_2\ddot{e} + \dddot{e} = c_1\dot{e} + c_2\ddot{e} + x_3 - \dddot{x}_{1d} \\ &= c_1\dot{e} + c_2\ddot{e} + \alpha(x) + bu - \dddot{x}_{1d} \\ &= c_1\dot{e} + c_2\ddot{e} + \alpha(x) - c_1\dot{\hat{e}} - c_2\ddot{\hat{e}} - \alpha(\hat{x}) - \eta\hat{s} + \dddot{x}_{1d} - \dddot{x}_{1d} \\ &= \eta\hat{s} + v(\tilde{x}) + \alpha(x) - \alpha(\hat{x}). \end{aligned} \tag{8}$$

To analyze the stability, a Lyapunov candidate function is defined as

$$V = \frac{1}{2}s^2. \tag{9}$$

The derivative of Lyapunov candidate function is presented as

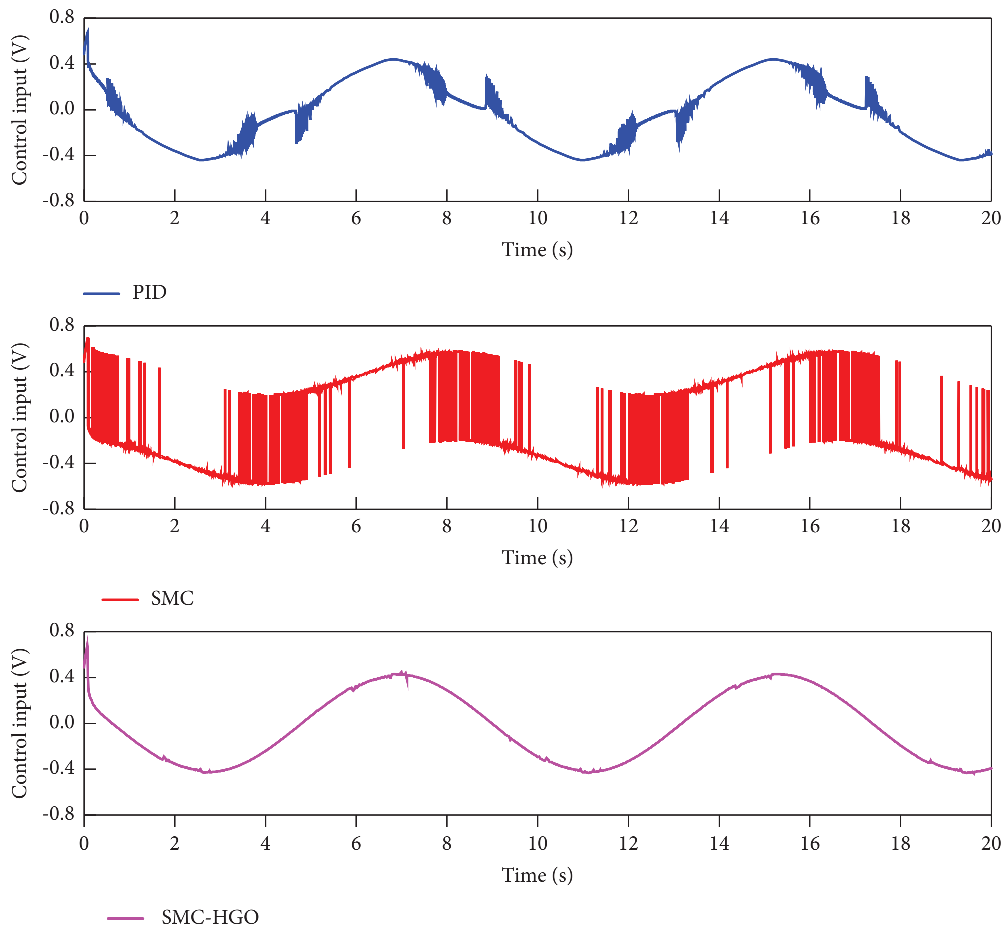

Figure 5: Control inputs of sinusoidal signal.

$$\begin{aligned}\dot{V} &= s\dot{s} = -\eta s\hat{s} + s\left(v(\tilde{x}) + \alpha(x) - \alpha(\hat{x})\right)\\ &= -\eta s\left(s - \tilde{s}\right) + s\left(v(\tilde{x}) + \alpha(x) - \alpha(\hat{x})\right)\\ &= -\eta s^2 + s\left(\eta\tilde{s} + v(\tilde{x}) + \alpha(x) - \alpha(\hat{x})\right)\\ &= -\eta s^2 + sf(\tilde{x}) \leq -\eta s^2 + \frac{1}{2}\left(sf(\tilde{x})^2\right)\\ &= -(\eta - 0.5)s^2 + 0.5f(\tilde{x})^2\\ &= -\eta_1 V + 0.5f(\tilde{x})^2,\end{aligned} \tag{10}$$

where $\eta_1 = 2\eta - 1$, $\tilde{x} = x - \hat{x}$, $f(x) = \eta\tilde{s} + v(\tilde{x}) + \alpha(x) - \alpha(\hat{x})$.

Theorem 1. *If $V \in R^+$, the solution of inequality equation $\dot{V} \leq -\sigma V + f, \forall t \geq t_0 \geq 0$ is*

$$V(t) \leq e^{-\gamma(t-t_0)}V(t_0) + \int_{t_0}^{t} e^{-\gamma(t-\tau)}f(\tau)\mathrm{d}\tau, \tag{11}$$

where γ is a constant.

Proof of theorem 1. Let $\Delta(t) = \dot{V}(t) + \gamma V(t) - f$, that is

$$\dot{V}(t) = -\gamma V(t) + f + \Delta(t). \tag{12}$$

According to the first order differential equation, the solution of equation (12) can be obtained as follows:

$$V(t) = e^{-\gamma(t-t_0)}V(t_0) + \int_{t_0}^{t} e^{-\gamma(t-\tau)}f(\tau)\mathrm{d}\tau + \int_{t_0}^{t} e^{-\gamma(t-\tau)}\Delta(\tau)\mathrm{d}\tau. \tag{13}$$

Due to $\forall t \geq t_0 \geq 0, \Delta(t) \leq 0$,

$$V(t) = e^{-\gamma(t-t_0)}V(t_0) + \int_{t_0}^{t} e^{-\gamma(t-\tau)}f(\tau)\mathrm{d}\tau. \tag{14}$$

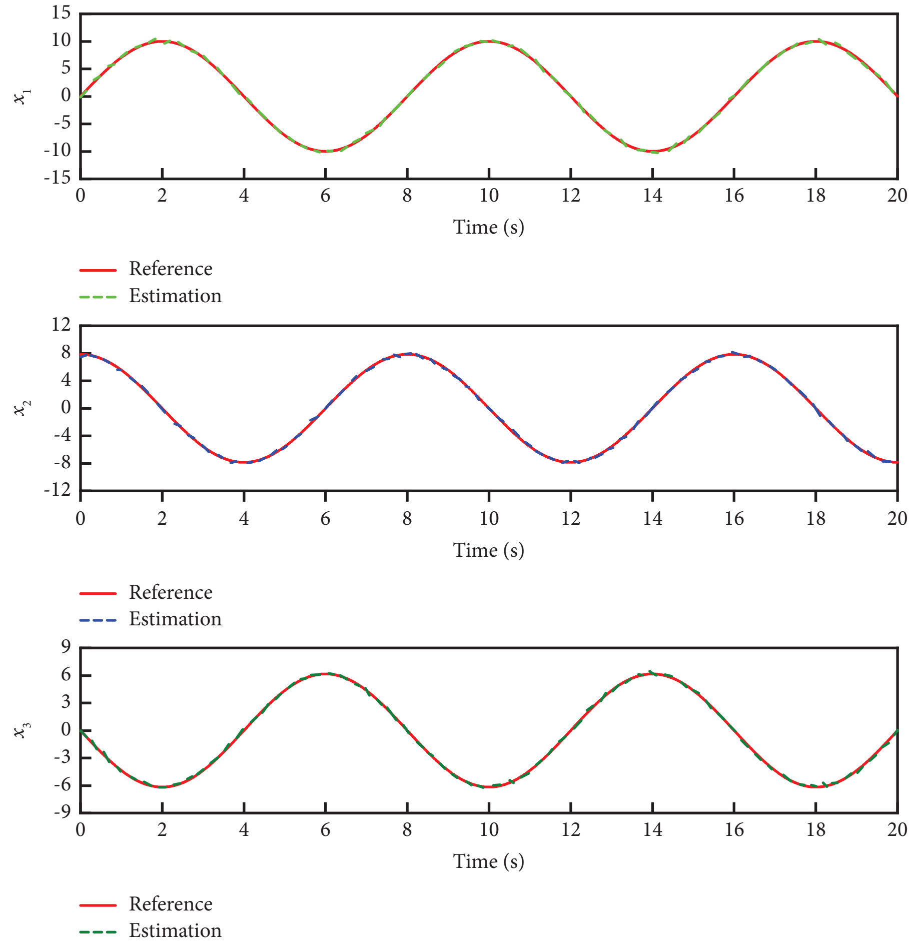

Figure 6: State variables estimation results of sinusoidal signal.

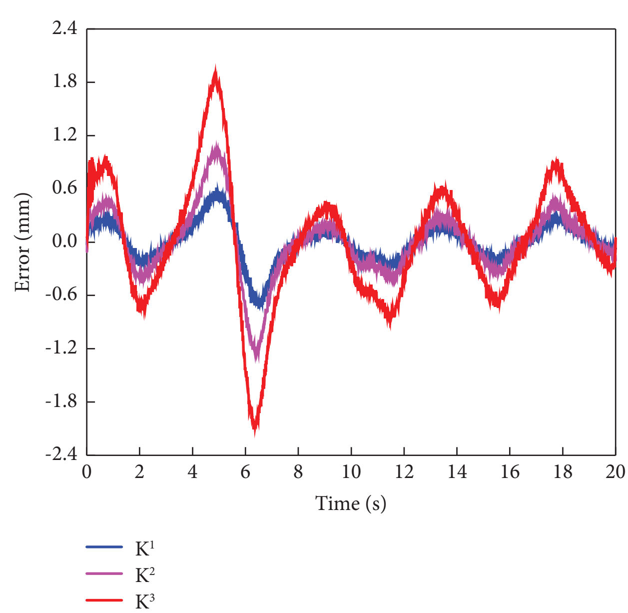

Figure 7: Comparison errors for different parameters of the proposed controller.

Table 1: Performance indices for sinusoidal signal.

Indices (mm)	μ	σ	E
PID	0.4238	0.3098	0.3523
SMC	0.2042	0.1644	0.1844
SMC-HGO	0.1507	0.1069	0.1361

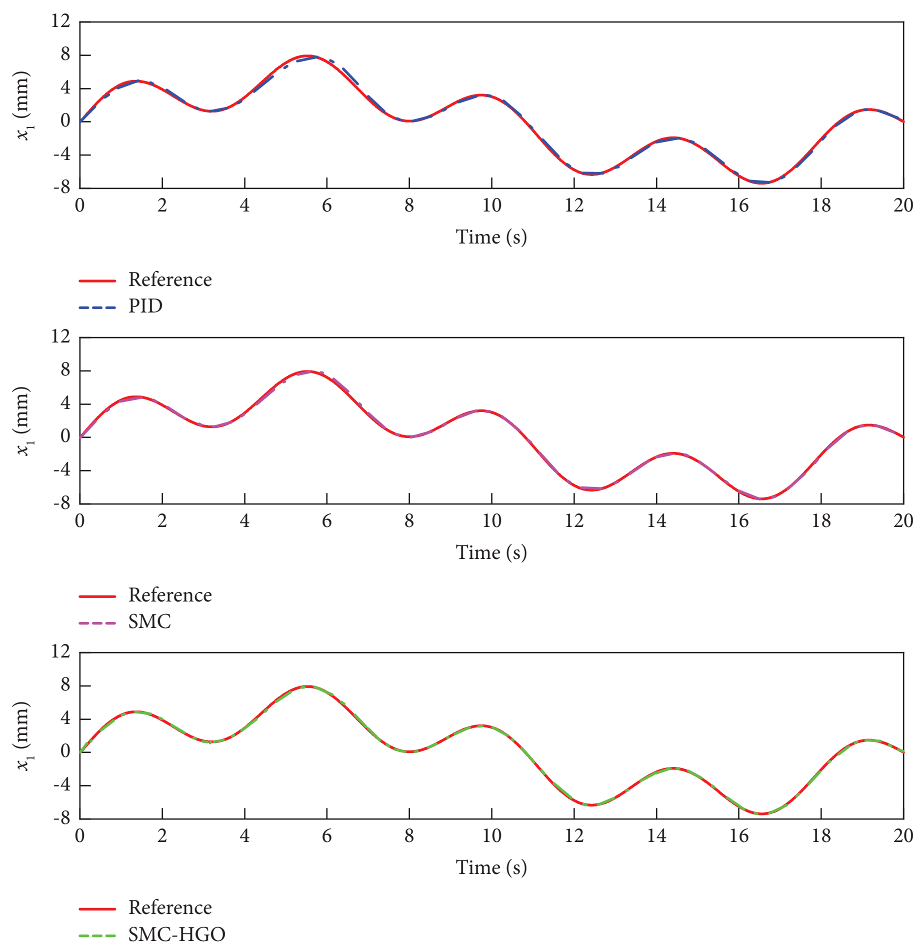

Figure 8: Comparative tracking performance of multifrequency sinusoidal signal.

Because $\tilde{x}$ is exponential convergence, we obtain $\|x(t)\| \leq \varphi_0 \|\tilde{x}(t_0)\| e^{-\sigma_0 (t-t_0)}$, then the equation (10) can be rearranged as

$$\dot{V}(t) = -\eta_1 V(t) + 0.5 f(\tilde{x})^2 \leq -\eta_1 V(t) + \chi(\bullet) e^{-\sigma_0 (\tau - t_0)}, \tag{15}$$

where $\chi(\bullet)$ is K-class function.

Combining equations (14) and (15), we have

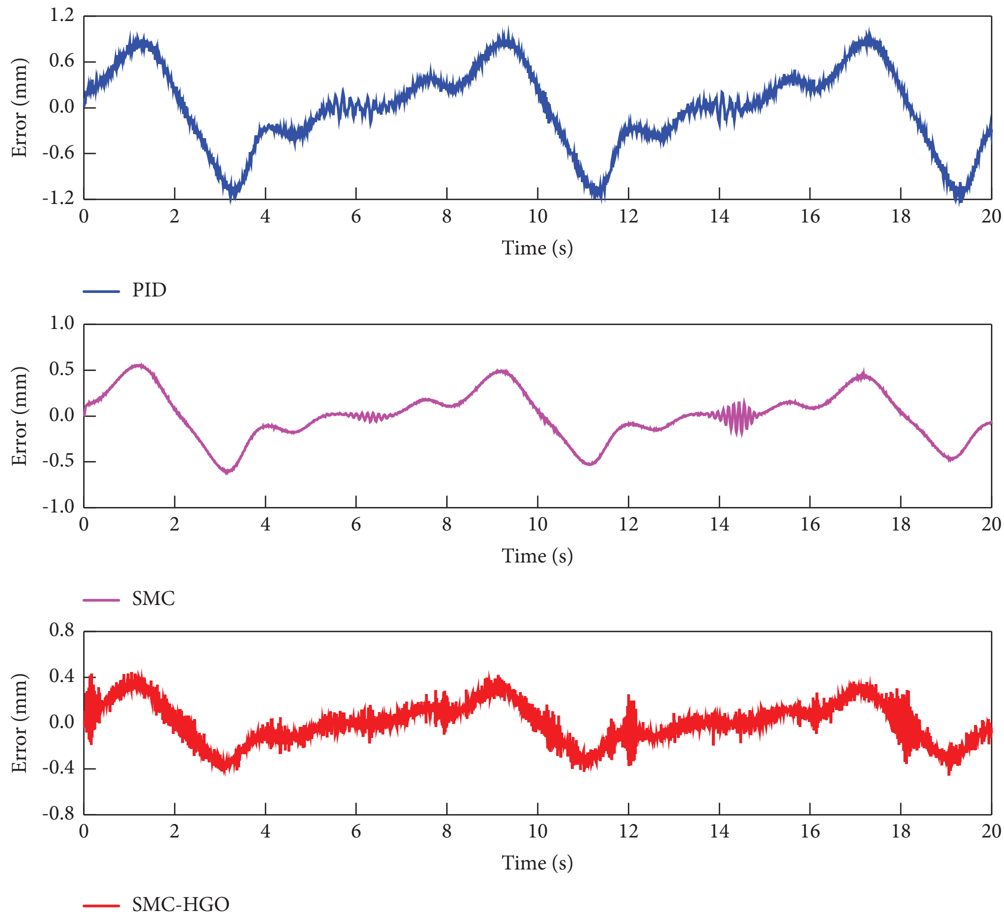

FIGURE 9: Comparative tracking errors of multifrequency sinusoidal signal.

$$\begin{aligned} V(t) &\leq e^{-\eta_1 (t-t_0)} V(t_0) + \chi(\bullet) \int_{t_0}^{t} e^{-\eta_1 (t-\tau)} e^{-\sigma_0 (\tau - t_0)} \mathrm{d}\tau \\ &= e^{-\eta_1 (t-t_0)} V(t_0) + \chi(\bullet) e^{-\eta_1 t + \sigma_0 t_0} \int_{t_0}^{t} e^{(\eta_1 - \sigma_0)\tau} \mathrm{d}\tau \\ &= e^{-\eta_1 (t-t_0)} V(t_0) + \frac{\chi(\bullet)}{(\eta_1 - \sigma_0)} e^{-\eta_1 t + \sigma_0 t_0} \left(e^{(\eta_1 - \sigma_0)t} - e^{(\eta_1 - \sigma_0)t_0} \right) \\ &= e^{-\eta_1 (t-t_0)} V(t_0) + \frac{\chi(\bullet)}{(\eta_1 - \sigma_0)} \left(e^{-\sigma_0 (t-t_0)} - e^{-\eta_1 (t-t_0)} \right). \end{aligned} \tag{16}$$

Thus, $t \longrightarrow \infty$, $V(t) = 0$, and $V(t)$ exponentially converge to zero. The accuracy convergence accuracy is determined by η_1.

Figure 2 shows the block diagram of the presented SMC-HGO control scheme. The proposed control scheme consists of a HGO and a SMC. The HGO is designed to estimate the velocity and the acceleration by using the position feedback signal. The SMC is proposed to improve the position tracking performance of the electro-hydraulic servo system. □

4. Simulation Results

To demonstrate the effectiveness of the proposed SMC-HGO control scheme, a classical PID controller and a SMC controller are conducted to compare with it. The controller parameters are defined as follows: (1) PID: The proportional gain $k_p = 1500$, the integral gain $k_i = 300$, and the differential gain $k_d = 0.2$. Especially, the gains of PID controller are selected by using the intelligent optimization algorithm for obtaining the excellent dynamic performance. (2) SMC:

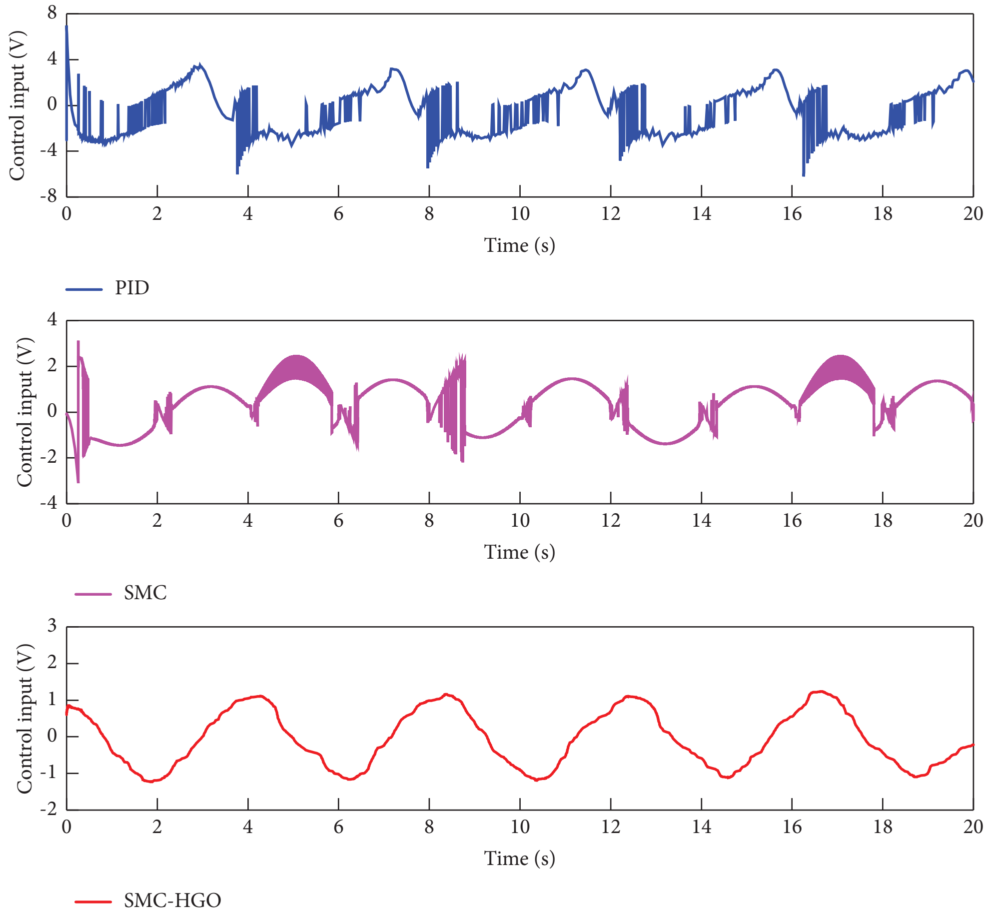

FIGURE 10: Control inputs of multifrequency sinusoidal signal.

$c_1 = 5$, $c_2 = 5$. (3) SMC-HGO:$c_1 = 5$, $c_2 = 5$, $k_1 = 20$, $k_2 = 50$, $k_3 = 100$, $\varepsilon = 0.01$, $\eta = 1.5$. The parameters of the electro-hydraulic servo system and controller are $m = 200\,\text{kg}$, $K = 1.5 \times 10^4\,\text{N/m}$, $B = 2 \times 10^3\,\text{N·s/m}$, $A = 2 \times 10^{-4}\,\text{m}^2$, $\rho = 800\,\text{kg/m}^3$, $C_{tc} = 2.5 \times 10^{-11}\,\text{m}^3/(\text{s·Pa})$, $V_t = 2 \times 10^{-4}\,\text{m}^3$, $\beta_e = 61.5 \times 10^3\,\text{bar}$, $C_d = 0.6$, $\varepsilon = 0.01$, $\eta = 0.5$, $c_1 = 5$, $c_2 = 3$, $h_1 = 0.5$, $h_2 = 0.8$, $h_3 = 0.4$. The sampling time for the simulation test is chosen as 1 ms.

The comparative tracking performance and errors for sinusoidal signal $y = 10\sin(0.25\pi t)$ are shown in Figures 3 and 4, respectively. As shown in Figure 3, three controllers can make the actuator of hydraulic cylinder follow the desired trajectory well. Specially, the maximum tracking errors of PID controller and SMC controller are 0.7 mm and 0.5 mm, respectively. In contrast, the tracking error of SMC-HGO is only 0.4 mm, which validates the superiority of the proposed control scheme. The comparison of control inputs signal is shown in Figure 5. It can be noted that control input of SMC is changed drastically due to the inherent chattering characteristic. Compared with SMC, the SMC-HGO has smooth control input signal, which is due to its ability to compensate for lumped uncertainties. The state variables estimation results of the proposed method are shown in Figure 6. It can be seen from Figure 6 that the estimated states track the reference states quite well, which validates the estimation accuracy of the high gain observer. The aforementioned simulations reveal that the presented controller has better tracking performance than SMC and smaller chattering in control action, which is very important for high performance control of the electro-hydraulic servo system. Since the HGO is very critical for the presented controller, three groups of HGO gains are chosen as follows: $K^1 = [k1,\ k2,\ k3] = [20,\ 50,\ 100]$, $K^2 = 0.1\,K^1$, and $K^3 = 10\,K^1$. Comparison errors between the reference and the response for different parameters of the proposed controller are shown in Figure 7. It is clear that the tracking performance can be improved by increasing the gains of HGO. However, too large HGO gains will lead to a larger error.

In addition, three quantitative performance indices, i.e., the average value of absolute error μ, the standard deviation of absolute error σ, and integral of time multiplied by error E are adopted to evaluate the abovementioned controllers. Performance indices for sinusoidal signal are listed in Table 1. It shows that the SMC-HGO outperforms the other two controllers in terms of all performance indices.

To further validate the performance of the presented controller, multifrequency sinusoidal signal $y = 5\sin(0.1\pi t) + 3\sin(0.45\pi t)$ is conducted. Comparative tracking performance and errors of three controllers are shown in Figures 8 and 9, respectively. It is shown that the presented controller has the better tracking accuracy

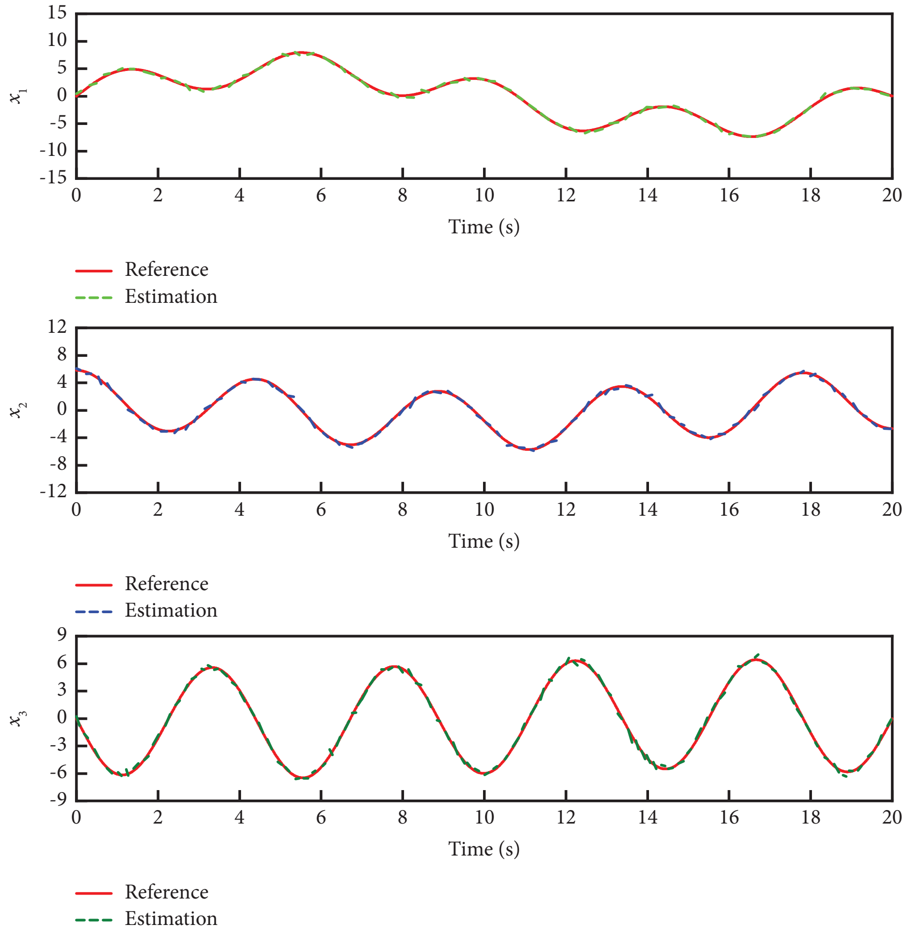

FIGURE 11: State variables estimation results of multifrequency sinusoidal signal.

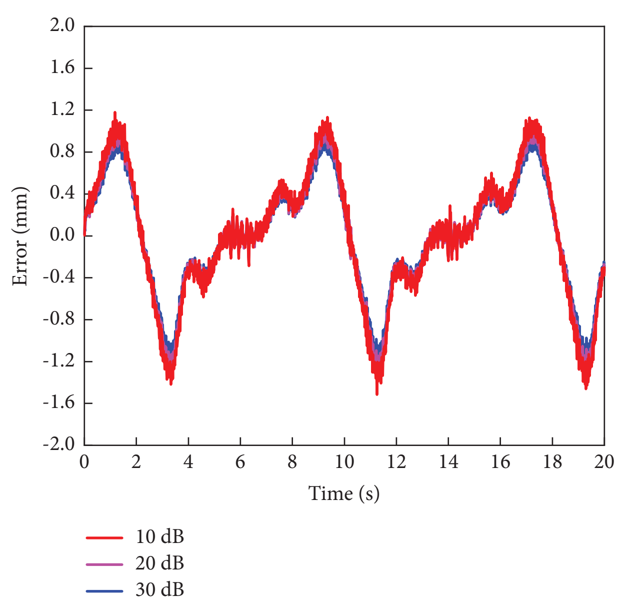

FIGURE 12: Comparative tracking errors of multifrequency sinusoidal signal under different SNR.

compared with PID controller and SMC controller. This is because the high gain observer is introduced in controller design to estimate the unmeasurable velocity and acceleration signal. The comparative control inputs signal of three controllers is displayed in Figure 10. It is clear that the presented control method is smoother than

Table 2: Performance indices for multifrequency sinusoidal signal.

Indices (mm)	μ	σ	E
PID	0.0166	0.0142	0.0154
SMC	0.0097	0.0088	0.0095
SMC-HGO	0.0080	0.0065	0.0078

that of the other two controllers, which shows that the SMC-HGO provides superior control performance than PID and SMC schemes. State variables estimation results can be found in Figure 11. It can be found that the reference state variable is accurately estimated by the high gain observer. To study the antiuncertainty of the presented controller, the comparative tracking errors of multifrequency sinusoidal signal under the different signal-noise ratio (SNR) are displayed in Figure 12. The tracking error is related to the SNR. The larger the SNR is, the lower the tracking performance accuracy is. However, the compared tracking errors of the three SNR are acceptable, which further verifies the powerful capability of the presented controller in suppressing lumped uncertainties.

The performance indices for multifrequency sinusoidal signal are summarized by Table 2. Especially, the σ of the presented controller is 0.0065 mm, while the corresponding values of the PID controller and SMC controller are 0.0142 mm and 0.0088 mm, respectively. It can be easily known that the SMC-HGO has a better tracking performance than the other two controllers.

5. Conclusion

In this paper, a novel SMC-HGO is presented for the electro-hydraulic servo system. The dynamic model is first constructed, where the parameter uncertainties and external disturbances are regarded as lumped uncertainties. The HGO is introduced to obtain accurate velocity and acceleration signal. The stability analysis carried by the Lyapunov method displays an exponential convergence performance. Then, the comparative simulations are illustrated both in different reference signals and controller parameters. The results show the superior tracking performance of the SMC-HGO with high tracking precision and chattering-free in the tracking control of the electro-hydraulic servo system.

Data Availability

The data used to support the findings of this study are included within the article.

Conflicts of Interest

The authors declare that they have no conflicts of interest.

Acknowledgments

The work is supported by the Key Science and Technology Program of Henan Province (Grant no. 222102220104), the Science and Technology Key Project Foundation of Henan Provincial Education Department (Grant no. 23A460014) and the High Level Talent Foundation of Henan University of Technology (Grant no. 2020BS043).

References

[1] Q. Guo and Z. L. Chen, “Neural adaptive control of single-rod electrohydraulic system with lumped uncertainty,” *Mechanical Systems and Signal Processing*, vol. 146, Article ID 106869, 2021.

[2] G. Shen, Z. C. Zhu, X. Li, Q. G. Wang, G. Li, and Y. Tang, “Acceleration waveform replication on six-degree-of-freedom redundant electro-hydraulic shaking tables using an inverse model controller with a modelling error,” *Transactions of the Institute of Measurement and Control*, vol. 40, no. 3, pp. 968–986, 2018.

[3] S. Chen, Z. Chen, B. Yao et al., “Adaptive robust cascade force control of 1-DOF hydraulic exoskeleton for human performance augmentation,” *IEEE-ASME Transactions on Mechatronics*, vol. 22, no. 2, pp. 589–600, 2017.

[4] W. X. Deng, J. Y. Yao, Y. Y. Wang, X. W. Yang, and J. H. Chen, “Output feedback backstepping control of hydraulic actuators with valve dynamics compensation,” *Mechanical Systems and Signal Processing*, vol. 158, pp. 107769–107818, 2021.

[5] Y. Ge, J. Zhou, W. Deng, J. Yao, and L. Xie, “Neural network robust control of a 3-DOF hydraulic manipulator with asymptotic tracking,” *Asian Journal of Control*, 2022.

[6] S. B. Wang and J. Na, “Parameter estimation and adaptive control for servo mechanisms with friction compensation,” *IEEE Transactions on Industrial Informatics*, vol. 16, no. 11, pp. 6816–6825, 2020.

[7] S. A. Nahian, D. Q. Truong, P. Chowdhury, D. Das, and K. K. Ahn, “Modeling and fault tolerant control of an electro-hydraulic actuator,” *International Journal of Precision Engineering and Manufacturing*, vol. 17, no. 10, pp. 1285–1297, 2016.

[8] X. D. Li, X. Chen, and C. S. Zhou, “Combined observer-controller synthesis for electro-hydraulic servo system with modeling uncertainties and partial state feedback,” *Journal of the Franklin Institute*, vol. 355, no. 13, pp. 5893–5911, 2018.

[9] M. Van, X. P. Do, and M. Mavrovouniotis, “Self-tuning fuzzy PID-nonsingular fast terminal sliding mode control for robust fault tolerant control of robot manipulators,” *ISA Transactions*, vol. 96, pp. 60–68, 2020.

[10] X. Yang, W. Deng, L. Liu, and J. Yao, “A novel adaptive-gain disturbance estimator-based asymptotic adaptive tracking control for uncertain nonlinear systems,” *Transactions of the Institute of Measurement and Control*, vol. 44, no. 5, pp. 1045–1055, 2022.

[11] W. X. Deng and J. Y. Yao, “Adaptive integral robust control and application to electromechanical servo systems,” *ISA Transactions*, vol. 67, pp. 256–265, 2017.

[12] J. Y. Yao, Z. X. Jiao, and D. W. Ma, “Adaptive robust control of DC motors with extended state observer,” *IEEE Transactions on Industrial Electronics*, vol. 61, no. 7, pp. 3630–3637, 2014.

[13] Q. Guo, Y. L. Liu, D. Jiang et al., “Prescribed performance constraint regulation of electrohydraulic control based on backstepping with dynamic surface,” *Applied Sciences*, vol. 8, no. 1, pp. 76–16, 2018.

[14] X. B. Yang, X. L. Zheng, and Y. H. Chen, “Position tracking control law for an electro-hydraulic servo system based on backstepping and extended differentiator,” *IEEE-ASME Transactions on Mechatronics*, vol. 23, no. 1, pp. 132–140, 2018.

[15] C. G. Yang, Y. M. Jiang, J. Na, Z. J. Li, L. Cheng, and C. Y. Su, "Finite-time convergence adaptive fuzzy control for dual-arm robot with unknown kinematics and dynamics," *IEEE Transactions on Fuzzy Systems*, vol. 27, no. 3, pp. 574–588, 2019.

[16] C. E. Ren, S. C. Tong, and Y. M. Li, "Fuzzy adaptive high-gain-based observer backstepping control for SISO nonlinear systems with dynamical uncertainties," *Nonlinear Dynamics*, vol. 67, no. 2, pp. 941–955, 2012.

[17] C. Y. Li, S. C. Tong, and W. Wang, "Fuzzy adaptive high-gain-based observer backstepping control for SISO nonlinear systems," *Information Sciences*, vol. 181, no. 11, pp. 2405–2421, 2011.

[18] Y. Zhang, S. Li, and X. Liu, "Neural network-based model-free adaptive near-optimal tracking control for a class of nonlinear systems," *IEEE Transactions on Neural Networks and Learning Systems*, vol. 29, no. 12, pp. 6227–6241, 2018.

[19] Z. Chen, F. H. Huang, W. C. Sun, J. Gu, and B. Yao, "RBF-Neural-Network-Based adaptive robust control for nonlinear bilateral teleoperation manipulators with uncertainty and time delay," *IEEE-Asme Transactions on Mechatronics*, vol. 25, no. 2, pp. 906–918, 2020.

[20] W. M. Bessa, M. S. Dutra, and E. Kreuzer, "Sliding mode control with adaptive fuzzy dead-zone compensation of an electro-hydraulic servo-system," *Journal of Intelligent and Robotic Systems*, vol. 58, no. 1, pp. 3–16, 2010.

[21] Y. Y. Wang, S. R. Jiang, B. Chen, and H. T. Wu, "A new continuous fractional-order nonsingular terminal sliding mode control for cable-driven manipulators," *Advances in Engineering Software*, vol. 119, pp. 21–29, 2018.

[22] S. Q. Zhu, X. L. Jin, B. Yao, Q. C. Chen, X. Pei, and Z. Q. Pan, "Non-linear sliding mode control of the lower extremity exoskeleton based on human-robot cooperation," *International Journal of Advanced Robotic Systems*, vol. 13, no. 5, pp. 172988141666278–10, 2016.

[23] J. Y. Yao, W. X. Deng, and Z. X. Jiao, "Adaptive control of hydraulic actuators with LuGre model-based friction compensation," *IEEE Transactions on Industrial Electronics*, vol. 62, no. 10, pp. 6469–6477, 2015.

[24] Q. Guo, Y. Zhang, B. G. Celler, and S. W. Su, "Backstepping control of electro-hydraulic system based on extended-state-observer with plant dynamics largely unknown," *IEEE Transactions on Industrial Electronics*, vol. 63, no. 11, pp. 6909–6920, 2016.

[25] W. Kim, D. Won, D. Shin, and C. C. Chung, "Output feedback nonlinear control for electro-hydraulic systems," *Mechatronics*, vol. 22, no. 6, pp. 766–777, 2012.

[26] G. Yang, J. Yao, and Z. Dong, "Neuroadaptive learning algorithm for constrained nonlinear systems with disturbance rejection," *International Journal of Robust and Nonlinear Control*, vol. 32, no. 10, pp. 6127–6147, 2022.

[27] G. Yang, J. Yao, and N. Ullah, "Neuroadaptive control of saturated nonlinear systems with disturbance compensation," *ISA Transactions*, vol. 122, pp. 49–62, 2022.

[28] L. Liu, Y.-J. Liu, and S. Tong, "Neural networks-based adaptive finite-time fault-tolerant control for a class of strict-feedback switched nonlinear systems," *IEEE Transactions on Cybernetics*, vol. 49, no. 7, pp. 2536–2545, 2019.

[29] W. Shen, J. H. Wang, H. L. Huang, and J. Y. He, "Fuzzy sliding mode control with state estimation for velocity control system of hydraulic cylinder using a new hydraulic transformer," *European Journal of Control*, vol. 48, pp. 104–114, 2019.

[30] G. Palli, S. Strano, and M. Terzo, "Sliding-mode observers for state and disturbance estimation in electro-hydraulic systems," *Control Engineering Practice*, vol. 74, pp. 58–70, 2018.

[31] C. Cheng, S. Y. Liu, and H. Z. Wu, "Sliding mode observer-based fractional-order proportional-integral-derivative sliding mode control for electro-hydraulic servo systems," *Proceedings of the Institution of Mechanical Engineers - Part C: Journal of Mechanical Engineering Science*, vol. 234, no. 10, pp. 1887–1898, 2020.

[32] D. Won, W. Kim, and M. Tomizuka, "High-gain-observer-based integral sliding mode control for position tracking of electrohydraulic servo systems," *IEEE-ASME Transactions on Mechatronics*, vol. 22, no. 6, pp. 2695–2704, 2017.